Limits on nonstandard weak currents from the polarization of ^{14}O and ^{10}C decay positrons

A. S. Carnoy, J. Deutsch, T. A. Girard,* and R. Prieels
Institut de Physique Nucléaire, Université Catholique de Louvain, 1348 Louvain-la-Neuve, Belgium
(Received 16 November 1990)

We report the relative polarization of the $P_F/P_{GT}=0.9996\pm0.0037$ for the positrons emitted by the pure Fermi ^{14}O and the pure Gamow-Teller ^{10}C decays, using a technique based on the observation of the positronium-decay time spectrum. The radioisotopes to be compared are part of the same source, eliminating some of the potential systematic errors which may vitiate relative polarization measurements of high precision. Combining our result with a similar $^{26}Al^m/^{30}P$ decay positron comparison obtained by Bhabha polarimetry, we deduce the following constraint on the product of the mixing angle ζ and mass-squared ratio δ of the chiral W bosons assumed in left-right symmetric models: $-0.0004<\zeta\delta<0.0007$ (90% C.L.). Our result also constrains possible scalar and tensor admixtures to the dominant vector and axial-vector currents:

$$\frac{C_S+C_S'}{C_V}-\frac{C_T+C_T'}{C_A}=0.003\pm0.018 \text{ (90\% C.L.)} .$$

I. INTRODUCTION

Parity symmetric extensions of the standard $SU(2)_L\times U(1)$ model have attracted considerable attention in recent years.[1] Such models, based on the gauge group $SU(2)_L\times SU(2)_R\times U(1)$, are characterized by an additional, predominantly right-handed, charged gauge boson W_1, which, as a consequence of spontaneous symmetry breaking, acquires a larger mass than the observed predominantly left-handed boson W_1. This accounts for the predominance of left-handed couplings at low energies, while restoring parity conservation at a higher-energy scale. In the minimal scenario of manifest left-right symmetry,[2-4] the only new parameters introduced into the description of the low-energy charged-current interaction are the mixing angle ζ and the mass-squared ratio $\delta=(M_1/M_2)^2$, where M_1 (M_2) is the mass of the predominantly left- (right-) handed gauge boson ($M_1=81$ GeV/c^2, $M_1\ll M_2$). The physical bosons of well-defined mass, W_1 and W_2, are related to the states W_L and W_R which couple to the left- and right-handed fermion currents by $W_1=W_L\cos\zeta-W_R\sin\zeta$ and $W_2=W_L\sin\zeta+W_R\cos\zeta$. Extensions of this minimal model will be considered in Sec. VI.

Limits on the admixture of right-handed currents have been obtained from the measured ratio $R=P_F/P_{GT}$ of the polarizations of positrons emitted in Fermi (P_F) and Gamow-Teller decays (P_{GT}), which is a function of ζ and δ:

$$R=(1+\varepsilon^2\delta)(\varepsilon^2+\delta^2)(1+\varepsilon^2\delta^2)^{-1}(\varepsilon^2+\delta)^{-1} , \quad (1)$$

with $\varepsilon=(1+\tan\zeta)/(1-\tan\zeta)$.[5-7] To first order in ζ and δ, this expression becomes $R=1+8\zeta\delta$. Neglecting recoil-order corrections, which are small in our case, the standard model predicts $\zeta=\delta=0$, i.e., $R=1$.

In the absence of right-handed vector and axial-vector currents, our result also constrains the Fierz interference terms, i.e., the admixture of anomalous scalar or tensor couplings into the canonical $V-A$ theory. This results from the fact that the positron polarization is related to the Fierz term b,[8] which contains the scalar admixture to the vector coupling in the case of pure Fermi decay (b_F) and the tensor admixture to the axial-vector coupling in the case of pure Gamow-Teller decay (b_{GT}). Assuming the couplings are real, and in the absence of right-handed currents for the vector and axial-vector interactions ($C_V=C_V'$ and $C_A=C_A'$), the polarization ratio $R=P_F/P_{GT}$ is a simple function of b_F and b_{GT}:

$$R-1=\frac{m_e}{E}(b_F-b_{GT}) , \quad (2)$$

where $b_F=(C_S+C_S')/C_V$, $b_{GT}=(C_T+C_T')/C_A$, m_e is the positron mass, and E the positron energy.

Finally, our result may be used to constrain exotic processes such as leptoquark exchange, which would also influence polarization in semileptonic transitions;[9] we will not expand upon this point.

We performed a precision measurement of the relative longitudinal polarization (R) of positrons emitted by ^{14}O (pure Fermi transition) and ^{10}C (pure Gamow-Teller transition), using a polarimeter based on time-resolved spectroscopy of hyperfine positronium (Ps) decay.[10-13] The two radioisotopes to be compared are part of the same source; by this innovation we avoid some of the systematic errors which may vitiate relative measurements pursued to their highest state-of-art precision. In what follows we report the details of this experiment, which was briefly described in a letter.[14]

II. DESCRIPTION OF THE EXPERIMENT

The experiment was performed using the on-line positron polarimeter of Louvain-la-Neuve shown schemati-

cally in Fig. 1 and located at the isochronous cyclotron of the university. The device consists of a source activation and transport system, a two-lens magnetic β spectrometer of asymmetric field (cf. Sec. II B), and the polarimeter. The entire operation of the instrument (the transport of the activated target, the polarimeter field change, and the CAMAC-based data acquisition) is under the control of a μ-Vax computer.

A. Production of the ^{10}C and ^{14}O isotopes

The positron-emitting radioisotopes ^{14}O and ^{10}C are produced by (p,n) reactions in the same target (a 140-mg/cm^2 BN compressed powder pellet, enriched to 90% in ^{10}B). The mixed nature of the target minimizes any differential depolarization of the positrons in the source. Protons of 21 MeV and 6-μA beam intensity are degraded to 14.5 MeV by a carbon foil before entering the BN target, in which they lose 4.5 MeV. The depth profile of both activities and the depolarizing power of BN were carefully measured to ascertain that the differential influence of this effect was in the 10^{-4} range (cf. Sec. IV).

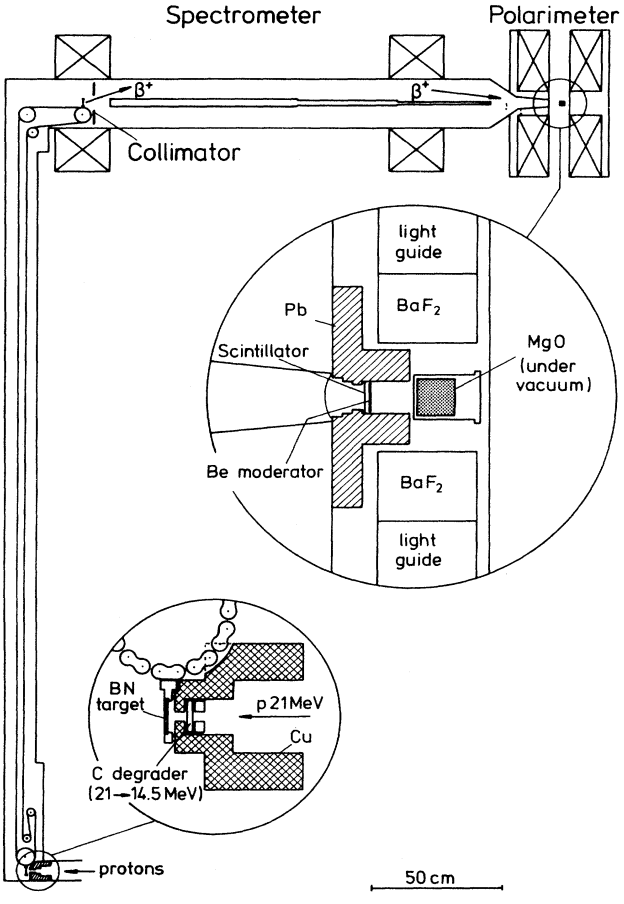

FIG. 1. UCL on-line positron polarimeter system: activation site (small inset), target transport system, spectrometer, and polarimeter (large inset).

B. Selection of the positrons

After irradiation the target is transported in 6 s to the focal point of the spectrometer, which selects 1.24-MeV positrons, with a momentum resolution of 12.5% full width at half maximum (FWHM). In addition to selecting the momenta, the spectrometer transports a maximum number of positrons to the polarimeter entrance as a beam that is near parallel to the field axis. This is accomplished by two iron-free coils aligned on the polarimeter axis in an asymmetric configuration similar to the one described in Ref. 15. The first coil, centered at the source location, is operated at 1.1 kG to provide an acceptance angle between 4° and 40°; the second, adjacent to the polarimeter entrance aperture, provides a 0.33-kG field to refocus the positrons into a nearly parallel beam. For conversion electrons, 3% of the electrons emitted by a source located at the target position are effectively injected into the polarimeter. For β emitters such as ^{14}O and ^{10}C, which emit positrons with a continuous energy spectrum of about 1.8-MeV end point, $\sim$0.3% of all emitted positrons are focused into the polarimeter if the spectrometer is adjusted to 1.24 MeV. Let us note that, for this energy, the inversion of the polarimeter field direction changes the injection efficiency by roughly 7%. The internal surfaces of the spectrometer are covered with rough-surfaced low-Z material in order to minimize scattering effects.

C. Polarimeter technique

Positrons which enter the magnet-gap region of the polarimeter sequentially cross a 0.4-mm-thick NE104 plastic START scintillator and a 1-mm beryllium moderator; they stop in a MgO powder pellet placed in vacuum, in which a 43% fraction forms Ps, the remainder annihilating directly. The essentials of the polarimeter operation, based on observation of the hyperfine Ps-decay time spectrum, have been described previously[11–13] and will be repeated here briefly.

In a field-free vacuum, Ps exists in two states:[16] a singlet state ($\tau_S = 0.125$ ns) and a triplet state ($\tau_T \approx 140$ ns). In a magnetic field, the ($m = \pm 1$) triplet substates remain unperturbed, but the ($m = 0$) triplet substate and singlet state are mixed to form two field-perturbed states. The three resulting states are then the perturbed singlet (PS), the perturbed triplet (PT), and the unperturbed triplet (T). Our polarimeter technique is based on the fact that both the PS and PT populations are functions of the relative directions of the magnetic field (**B**) and that of the longitudinal positron polarization (**P**). These populations are proportional to $(1 \pm \varepsilon P)$, respectively, to $(1 \mp \varepsilon P)$, where the upper sign corresponds to **B** parallel to **P** and the lower sign to the antiparallel case. We have $\varepsilon = x/(1+x^2)^{1/2}$, where $x \approx B(\text{kG})/36.3$. P is the residual longitudinal polarization of the positrons projected on the symmetry axis of the polarimeter, as they form Ps. The asymmetry in the PT population εP increases when the magnetic-field intensity is increased; on the other hand, the PT lifetime decreases:[16]

$$\lambda_{PT} = (\lambda_T + y^2 \lambda_S)/(1+y^2) ,$$

where λ_{PT}, λ_T, and λ_S are the decay rates of the PT, T, and S states, and $y = x/[1+(1+x^2)^{1/2}]$, with x defined as above. Consequently, the choice of the field to be used has to compromise between the size of the effect and the difficulty in separating the PT component of short lifetime. The polarimeter was operated at $B = 9.7$ kG, yielding $\varepsilon \approx 0.258$ and a PT lifetime of 7.267 ± 0.003 ns, in good agreement with theory. The inhomogeneity of the magnetic field in the PS-formation medium was less than 0.2% in the transverse direction and less than 1% in the longitudinal one.

Since the positron depolarization during the slowing down is proportional to the charge Z of the medium,[17] a 1-mm-thick beryllium degrader was placed just upstream of the powder chamber entrance window so as to increase the residual polarization upon stopping. This resulted in an increase of a factor (1.16 ± 0.03) in the measured asymmetry, which became $\varepsilon P = 14\%$. This Be degrader was also useful in minimizing the backscattering of positrons into the START detector.

D. Positronium-formation medium

The Ps-formation medium was selected on the basis of extensive tests of various MgO and SiO_2 powders characterized by different granulometries and provided by various manufacturers. Different conditioning procedures were also tested. The aim was to maximize the Ps-formation fraction and minimize the quenching. As a result, we selected an MgO powder [provided by E. Merck (Ref. 5862), D-1600 Darmstadt, Germany], characterized by a grain diameter of about 100 Å, compressed to 0.33 g/cm^3, and heat treated in vacuum to 300 °C for several hours in order to remove oxygen and water. This powder yielded a Ps triplet ($m = \pm 1$) lifetime of 128.2 ± 0.4 ns, only slightly less than the latest experimental vacuum value of 134 ns.[18] Furthermore, from the intensity of this component, we obtained an unquenched Ps-formation fraction of 43%. This value is roughly a factor of 2 larger than that achieved in other Ps-based polarimeters[15] and indicated that a sizable fraction of the Ps diffuses into the vacuum between the grains as a consequence of the small grain size. In the grains the Ps lifetimes are quenched to ~ 2 ns by the "pick-off" annihilation of the positron in an originally triplet state, with an electron of the medium.[19–21]

E. Detection system

The photons from Ps decay and direct annihilation are detected in two 5.1 cm diam × 3.8 cm BaF_2 STOP scintillators mounted in the polarimeter magnet housing at 180° to each other in a plane perpendicular to the field axis; for the 511-keV annihilation radiation, the combined detection efficiency of the detectors is 0.18 per positron annihilation into two photons. We used the fast component of the BaF_2 scintillation, of about 0.6 ns lifetime. A lead collimator was placed between the START and the STOP detectors (Fig. 1) in order to reduce by a factor of 10 the detection efficiency for photons of Ps formed in the START scintillator; the contribution of these spurious decays of 2.5 ns lifetime was reduced to 1% of all detected photons. Each STOP scintillator was coupled to a magnetically shielded XP2020Q photomultiplier located outside the polarimeter field region through a 30-cm quartz (Suprasil 1, provided by Heraeus Gmbh, Hanau) light guide. The START scintillator was edge coupled with Lucite to a magnetically shielded XP2020 photomultiplier. The timing signals were obtained using ORTEC 934 constant fraction timing discriminators without intermediate amplification of the photomultiplier signals. The two STOP channels were individually time aligned to within 15 ps and connected in OR logic. The time-resolved $\beta\gamma$-decay spectra were obtained from a fast time-to-digital converter of 156 ps channel width (LeCroy 4204 TDC), linked to an histogramming memory unit (LeCroy 3588 HIST MEM). Timing calibration yielded a resolution of 1.3 ns (FWHM). The diagram of the electronics is schematized in Fig. 2. Three features merit particular attention: (1) the updating discriminator of the START channel selects incoming positrons which are not preceded by another one within 80 ns, (2) the discriminators of 1000 ns pulse width in the STOP channels protect the circuit against the numerous after pulses from the late decay component of the BaF_2 scintillators, and (3) the 400-ns dead time of the common STOP channel provides for the flatness of a pure accidental time spectrum. Note that, in order to avoid useless START signals for the TDC, the START and STOP connections have been inverted.

F. Measurement strategy

As the two isotopes have different lifetimes (^{10}C: $t_{1/2} = 19.3$ s; ^{14}O: $t_{1/2} = 70.6$ s), their relative contribu-

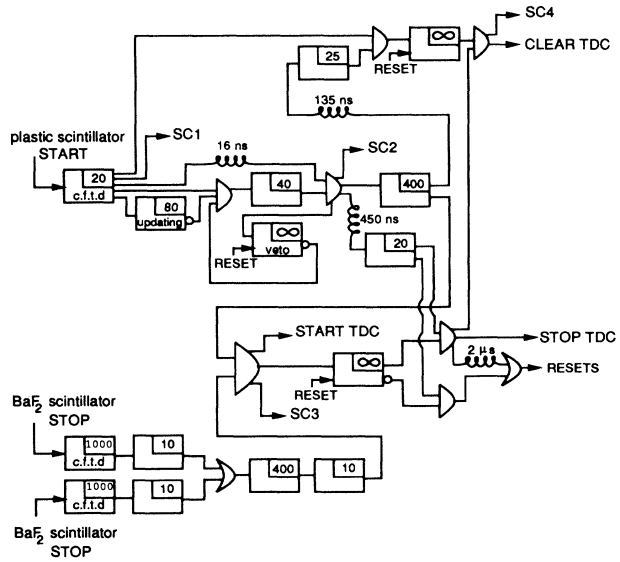

FIG. 2. Simplified diagram of the electronics. The scalers SCi measure the following quantities: SC1: β rate; SC2: rate of opened γ observation windows; SC3: $\beta\gamma$ rate; SC4: rate of β detected in a defined time window after the β-START. The signal widths are given in nanoseconds.

tions in the target change with time after the end of the irradiation; this feature allows a comparison of the polarization of the positrons emitted by the two isotopes. In order to determine both polarizations with near-equal instantaneous detection rates, measurements were performed in two kinds of cycles (Fig. 3): a short cycle (consisting of 7-s target activation, 6-s target transport, and 170 s during which the target stays in the spectrometer site) for a predominantly ^{10}C measurement and a long cycle (consisting of 70-s target activation, 30-s waiting, 6-s target transport, and 235 s during which the target stays in the spectrometer site) for a predominantly ^{14}O measurement. A sequence of one long and two short cycles was repeated, with the polarimeter field reversed every two cycles. In the short cycles, the $\beta\gamma$ time spectra were accumulated during the first 50 s succeeding the target arrival to the spectrometer site (window A; cf. Fig. 3); and in the long cycles, they were accumulated during the last 200 s of the cycle (window B; cf. Fig. 3). The β activity of the target, seen by the START detector, was observed in 1-s steps by multiscalers during the whole duration of the cycles; this allows the determination of the relative contributions of ^{10}C and ^{14}O, resolved on the basis of their characteristic lifetimes. The $\beta\gamma$ trigger rate was simultaneously stored in 1-s steps in order to determine the total dead time during the entire measurement.

The polarizations obtained from the $\beta\gamma$ time spectra stored during the windows A and B, respectively, P_A and P_B, are combinations of ^{10}C and ^{14}O polarizations. Denoting by f_A and f_B the fractions of pure Fermi positrons detected in the windows A and B,

$$P_A=(1-f_A)P_{GT}+f_AP_F ,$$

$$P_B=(1-f_B)P_{GT}+f_BP_F ,$$

where $f_A=0.272$ and $f_B=0.833$. The parameters f_A and f_B are determined on the basis of the relative contributions of both isotopes and of the contaminant ^{15}O (Table I). The relation between the measured ratio $K=P_B/P_A$ and $R=P_F/P_{GT}$ is given by

$$R=\frac{(f_A-1)K-(f_B-1)}{f_AK-f_B} . \quad (3)$$

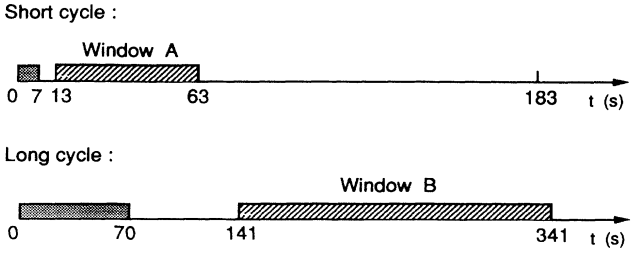

FIG. 3. Diagram of the time sequences characteristic of both types of cycles (short and long). The dashed regions correspond to the irradiation periods and the windows A or B in which the $\beta\gamma$-decay time spectra are stored. All the scalers are monitored during the entire cycle.

TABLE I. Percentage of the isotopes present in the observation windows A and B.

	Window A	Window B
^{10}C	(71.91±0.02)%	(15.30±0.02)%
^{14}O	(26.40±0.10)%	(79.08±0.52)%
^{15}O	(0.75±0.11)%	(4.07±0.60)%
^{11}C	(0.94±0.03)%	(1.55±0.10)%

Since K is approximately 1, the relation between the errors in K (σ_K) and in R (σ_R) is $\sigma_R\approx\sigma_K/(f_B-f_A)\approx 1.78\sigma_K$.

Instantaneous β rates ranged from 696 to 186 kHz in window A and from 768 to 86 kHz in window B. The motivation for this window strategy was to equalize in both measurements, as much as possible, the accidental $\beta\gamma$ coincidences (6.5% of all events in window A and 5.7% in window B) as well as the load on photomultipliers and electronics [see corrections (1) and (2) in Sec. IV]. With the short cycles twice as numerous as the long, the total statistics were similar in both windows.

The response function of the system was measured every 8 h by replacing the powder target with a stack of beryllium foils of similar macroscopic density and dimensions; as no Ps is produced in Be,[16] only prompt $\beta\gamma$ coincidences were present. Data were obtained over a total of 151 h: 123 h with MgO and 28 h with Be.

III. DATA ANALYSIS

Each $\beta\gamma$ time spectrum recorded during either MgO or Be cycles was corrected for accidental $\beta\gamma$ coincidences, of which there are three types: (a) the uncorrelated background which is observed at "negative" times, (b) coincidences where the observed photon is correlated with a β particle which preceded the β-START signal (these events are supressed by an electronic rejection of all β-START signals preceded by another β signal by less than 80 ns), and (c) coincidences where the observed photon is correlated with a β particle which penetrated the powder after the β-START signal. We did not reject electronically events of type (c) because such a rejection would have introduced a discontinuity in the decay time spectra a couple of ns after the prompt peak. Instead, the number of these events was deduced from β rate, $\beta\gamma$ rate, and the rate of β signals detected after the β-START in a well-defined temporal window (Fig. 2). Those rates were constantly monitored throughout the experiment (Fig. 3). The relative amounts of accidental events in the Ps-decay spectra measured in window A (B) was 3.0% (2.7%) and 24.1% (21.8%) at the beginning and the end of the adjustment region (3.8–62.2 ns after the direct annihilation peak), respectively.

Each corrected spectrum (corresponding to one cycle of measurement) was appropriately summed to yield the total decay spectra in each of the two (+,−) magnetic-field directions (Fig. 4) and for each measurement window (A and B). Here the + denotes **B** parallel to **P** and the −, **B** antiparallel to **P**. We then constructed the sum and the ratio (Fig. 4) of the spectra obtained for both field

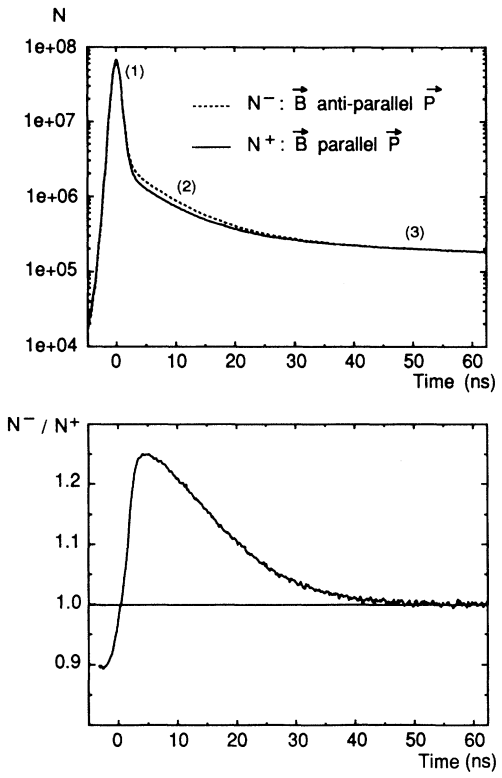

FIG. 4. (a) Total Ps-decay spectra (all data of the B window) measured with two opposite directions of the magnetic field: the spectrum N^+ (N^-) is measured with the field direction parallel (antiparallel) to the positron longitudinal polarization. We can clearly distinguish (1) the direct annihilation peak and the PS state of the Ps, (2) the PT state of the Ps, and (3) the T state of the Ps. (b) Ratio of the two spectra shown in (a): The maximum amplitude of this ratio ($\approx 2\varepsilon P$) shows the high analyzing power of our polarimeter.

directions, in the A and B windows. A fit was made simultaneously to these four spectra, convoluting the theoretical Ps-decay spectra with the measured response function. The four adjusted functions were $(M_A^- + M_A^+)$, $(M_B^- + M_B^+)$, (M_A^- / M_A^+), and (M_B^- / M_B^+), where the convoluted functions $M_{A/B}^{\pm}$ are defined as $M_{A/B}^{\pm} = T_{A/B}^{\pm} \otimes$(response function), and the expected Ps-decay spectra are

$$T_{A/B}^{\pm}(t) \propto \underbrace{(1-F)\delta(t)}_{\text{direct annihilation}} + \underbrace{\tfrac{1}{4}F(1 \pm \epsilon P_{A/B})\lambda_{\mathrm{PS}} e^{-\lambda_{\mathrm{PS}} t}}_{\text{perturbed singlet}} + \underbrace{\tfrac{1}{4}F(1 \mp \epsilon P_{A/B})\lambda_{\mathrm{PT}} e^{-\lambda_{\mathrm{PT}} t}}_{\text{perturbed triplet}} + \underbrace{\tfrac{1}{2}FS_{A/B}\lambda_{\mathrm{T}} e^{-\lambda_{\mathrm{T}} t}}_{\text{triplet}} + \underbrace{Q_{A/B}^{\pm}\lambda_Q e^{-\lambda_Q t}}_{\text{Ps in START scint}} . \quad (4)$$

The parameters common to all spectra were the T and PT lifetimes ($\lambda_{\mathrm{T}}^{-1}$ and $\lambda_{\mathrm{PT}}^{-1}$) and the Ps-formation fraction (F); those specific to the A and B windows were, in addition to the longitudinal polarization ($P_{A/B}$), the relative detection probability of the triplet decay into three photons ($S_{A/B}$) and the amplitude ($Q_{A/B}^{\pm}$) of a component of lifetime $\lambda_Q^{-1} = 2.5$ ns, corresponding to Ps formation in the START scintillator and MgO grains. This lifetime of 2.5 ns was determined in an independent experiment. The lifetime $\lambda_{\mathrm{PS}}^{-1}$ was fixed to its theoretical value of 0.125 ns.

The fit was made in a time region of 58.6 ns, beginning 3.8 ns after the direct annihilation peak since inclusion of the earlier portion would require introduction of additional parameters in Eq. (4) in order to describe, e.g., events due to backscattering. The lower limit of 3.8 ns was chosen on the basis of the evolution of the fit quality (χ^2) as a function of the first channel of the adjusted time interval (Fig. 5). As seen in Fig. 5, the final result is quite stable as a function of adjustments beginning later than 3.8 ns after $t = 0$. For the ratio of the polarizations in both measurement windows, we obtained $K = 1.0011 \pm 0.0020$ (statistical); the normalized χ^2 obtained in the adjustment of the ratios of $-$ and $+$ decay time spectra, which are sensitive to the polarization, is 1.3.

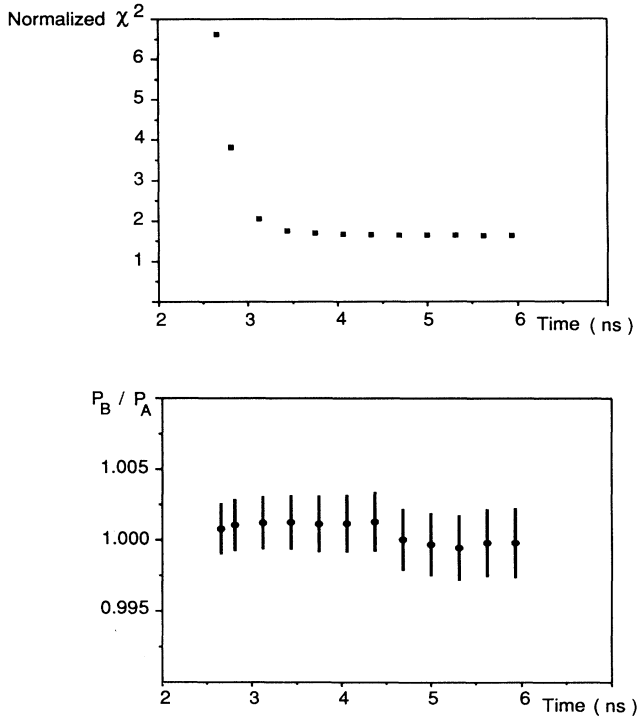

FIG. 5. (a) Normalized χ^2 obtained for the simultaneous adjustment of the sum and ratio of the positronium spectra measured in the two opposite directions of the magnetic field as a function of the beginning of the time region considered for the adjustment. (b) Result obtained for the polarization ratio $K = P_B / P_A$ in each adjustment reported in (a).

IV. SYSTEMATIC EFFECTS

The corrections and possible systematic errors of our experiment, with their contributions to the ratio K, are summarized in Table II and discussed below.

A. Accidental coincidences

The first correction on K given in Table II is induced by an error of $(2.1\pm0.2)\%$ in the calculation of the accidental coincidences of the type (c) discussed above. The correction to K is small compared with this error since the contributions of the accidental events are nearly equal in measurements A and B. This error in the calculation was checked in the Be experiments by considering the result of rejecting the $\beta\gamma$ coincidences each time a positron was detected in a region near the end of the observation window (Fig. 2, "CLEAR TDC"): The "gap" observed in the $\beta\gamma$ time spectrum at the place of this fast-clear window is sharp because in these experiments all the positrons annihilate directly, and its amplitude is a measure of the accidental coincidences. A typical time spectrum measured with a Be target is shown in Fig. 6: We observe the uncorrelated background for negative times and the accidental events of type (c) for positive times, with the well-defined gap discussed above.

B. Timing shifts

The mean timing shift between measurements performed in opposite field directions was 2 ps greater in window B than in window A. This shift was determined by fitting the ratio of the direct annihilation peaks to the ratio of two identical peaks shifted by known amounts. The impact of these shifts on K is quoted in Table II.

C. ^{11}C contribution

The measured polarizations in windows A and B were also corrected for a small ^{11}C contribution (Table II), formed by (p,n) activation of the 5% ^{11}B present in our enriched target and by (p,α) activation of the ^{14}N. Though the centroid of the spectrometer setting (1.24 MeV) was beyond the ^{11}C spectrum end point (0.96 MeV), 0.94% of the positrons in window A and 1.55% in window B originated from ^{11}C (Table I). The polarization of this impurity was measured in a separate experiment using a natural BN target (80% ^{11}B); it was 0.967 times the polarization obtained for ^{10}C and ^{14}O. The contribution of the mixed ^{15}O decay, of similar end-point energy as ^{10}C and ^{14}O, is not considered as a correction to K, but will be accounted for in the determination of R (Sec. V).

TABLE II. List of all corrections applied to the polarization ratio $K=P_B/P_A$, with their statistical errors.

(i) accidental coincidences	$(-0.14\pm0.02)\times10^{-3}$
(ii) timing shifts	$(-0.95\pm0.14)\times10^{-3}$
(iii) ^{11}C contribution	$(+0.23\pm0.61)\times10^{-3}$
(iv) ^{10}C/^{14}O target-depth difference: depolarization in target	$(-0.08\pm0.02)\times10^{-3}$
(v) ^{10}C/^{14}O end-point difference: depolarization upon stopping	$(-0.50\pm0.08)\times10^{-3}$
Total	$(-1.44\pm0.63)\times10^{-3}$

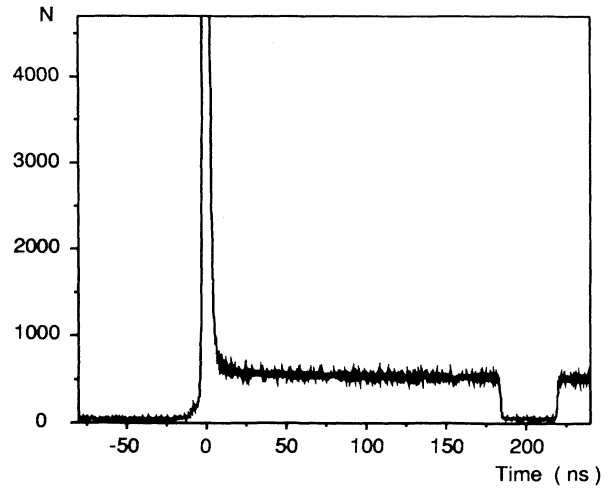

FIG. 6. Typical time spectrum measured with a Be target (12 min of acquisition time), with the direct annihilation peak truncated to $\frac{1}{200}$ of its amplitude. The uncorrelated background is observed at the left of the direct annihilation peak; at the right of the peak, we observe in addition events where the detected photon is correlated with a positron which penetrated the powder after the β-START; the gap corresponds to a time window in which those events were electronically rejected.

D. Differential depolarization in the target

The differential depolarization in the BN target between A and B measurements, because of the different spatial activity distribution of ^{10}C and ^{14}O in the target, induces a 10^{-4} level correction on K (Table II). This correction depends on the activity distribution in the target. In order to determine the distribution of both isotopes in the BN target, we measured the ^{10}B$(p,n)^{10}$C cross section relative to that of ^{14}N$(p,n)^{14}$O with a thin BN target (ΔE of protons=0.5 MeV), for protons of energy between 10 and 14.5 MeV. This cross-section ratio ranges from 2 to 3, and both distributions are quite similar: The mean locations differ only by $(0.85\pm0.02)\%$ of the target thickness (140 mg/cm^2). The positron depolarization in BN as a function of the target thickness crossed was determined by measuring the residual polarization of the positrons emitted by a ^{68}Ga source sandwiched between BN foils of variable thickness ranging from 0 to 140 mg/cm^2. Denoting by d the thickness of BN (in mg/cm^2) to be crossed by the positron in the target, we found a depolarization equal to $(-4.9\pm3.9)\times10^{-5}d$, yielding the correction reported in Table II.

E. Differential depolarization upon stopping

We considered also the differential depolarization upon stopping between windows A and B, due to the 3%

difference in the $^{10}C/^{14}O$ β spectrum end points (Table II). The characteristic energy spectrum of the positrons selected by the spectrometer was determined in each window using the spectrometer response function. This response function was measured with 0.976- and 1.048-MeV conversion electrons from ^{207}Bi. The energy dependence of the depolarization upon stopping was determined with positrons emitted by ^{68}Ga, measuring their residual polarization for selected energies ranging from 760 to 1240 keV. For the ratio of the residual polarizations at 760 and 1240 keV incident energy, corrected for the v/c factor, we found 1.21 ± 0.02. Note that Bouchiat and Lévy-Leblond[17] predicted a stronger energy dependence leading to a ratio 1.37.

Another systematic effect is introduced by possible differences in the scattering depolarization on the spectrometer walls, due to the difference in the β-spectrum end points of the two isotopes. In order to evaluate the contribution of this depolarization mechanism, we compared the experimental residual polarization of the positrons to that expected by taking into account (i) the depolarization in the BN target, experimentally determined as explained above, and (ii) the depolarization upon stopping in MgO, evaluated with the corrected approach of Bouchiat and Lévy-Leblond. The depolarization as a function of the incident energy, as calculated by Bouchiat and Lévy-Leblond was corrected by measuring the residual polarizations at incident energies E_i and E_j; we obtained the experimental ratios

$$[P(E_i)/P(E_j)]_{\text{expt}}=[1-\alpha f(E_i)]/[1-\alpha f(E_j)] ,$$

where α is a renormalization factor and the function $f(E)$ the depolarization computed by Bouchiat and Lévy-Leblond. We found $\alpha=0.76\pm0.07$. We then obtained an expected residual longitudinal polarization of $(38.9\pm5.2)\%$, where the error is due to the uncertainties on α and on the mean angle between the positron momentum and the longitudinal axis of the polarimeter. The experimental residual longitudinal polarization $(56.13\pm0.08)\%$ (the error is statistical) turned out to be slightly larger than the expected one, leaving no room for a sizable additional depolarization due to scattering on the walls. This observation seems to indicate that the depolarization upon stopping in MgO alone is similar to the one occurring partly during scattering on the walls and partly upon stopping in MgO. One could even argue that the observed residual polarization, slightly higher than the expected one, points toward a partial depolarization weaker in the spectrometer walls (covered by a material of low-Z value) than in the MgO pellet. As a consequence, we believe that the correction which takes into account the differential depolarization upon stopping in MgO (Table II) includes and even slightly overestimates the combined contribution of wall scattering and scattering in the MgO pellet.

V. CORRECTIONS ON P_F/P_{GT}

The polarization comparison between windows A and B is, after corrections, $K=0.9997\pm0.0021$. We extract from Eq. (3), on the basis of the relative quantities of $^{10}C/^{14}O$ in both windows (Table I),

$$R=P_F/P_{GT}=0.9996\pm0.0037 . \quad (5)$$

This value includes a small contribution of positrons emitted from ^{15}O (Table I) produced by (p,n) activation of ^{15}N (0.37% natural isotopic abundance). As the ^{15}O decay is a mixed transition, we applied the following relation to extract pure F and GT polarizations from its contribution:

$$P_{\text{mixed}}\approx\left[\frac{a^2}{a^2+c^2}\right]P_F+\left[\frac{c^2}{a^2+c^2}\right]P_{GT} ,$$

where a and c are the ^{15}O Fermi and Gamow-Teller form factors: $a^2=0.995\pm0.003$ and $c^2=0.406\pm0.005$.[22] Note that neglecting this ^{15}O contribution changes R by only 6×10^{-6}.

We have estimated the recoil order correction[23,24] to the ratio R on the basis of experimental information. The dominant recoil order term in our case is the so-called "weak magnetism" term in ^{10}C decay. Using the conserved vector current hypothesis, this is equal to the amplitude b_γ, related to the width of the analogous radiative transition $M1$ in ^{10}B by $\Gamma_{M1}=\frac{1}{6}\alpha E_\gamma^3 b_\gamma^2 M^{-2}$.[25] With $\Gamma_{M1}=\hbar/\tau$ and $\tau=7\pm3$ fs,[26] we obtain $|b_\gamma|=78.8\pm17.0$, which contributes a correction of $|(3.4\pm0.7)\times10^{-4}|$ to R. The sign of this small correction is, however, not known as the width is sensitive only to the square of the Gamow-Teller matrix element; for this reason, it has not been included in our final result for R.

VI. RESULT AND DISCUSSION

Our final result, $R=0.9996\pm0.0037$ [Eq. (5)], is comparable to the result of a similar $^{26}Al^m-^{30}P$ comparison[7] using fourfold Bhabba polarimetry, $R=1.003\pm0.004$, which, however, required a factor of 3 more counting time; this illustrates the merits of polarimeters based on time-resolved Ps spectroscopy. Note in this connection that our precision remains statistics limited: The combined error on all corrections is 3 times lower than the statistical error obtained in this experiment, leaving room for sizable improvements in precision.

The weighted average of both measurements is

$$P_F/P_{GT}=1.0010\pm0.0027 ,$$

providing the improved limit on the W_R parameters [cf. Eq. (1)] of

$$\zeta\delta=(1.3\pm3.4)\times10^{-4} . \quad (6)$$

This constitutes the best limit on right-handed current contributions to the weak interaction derived from β-polarization experiments to date. The technique of time-resolved Ps spectroscopy was also recently used by Skalsey *et al.*[15] to compare the positron polarization in the decays of $^{26}Al^m$ and ^{25}Al. However, because of the mixed character of the ^{25}Al transition, only the rather mild constraint of $\zeta\delta=(5\pm15)\times10^{-4}$ can be deduced from this measurement. The constraints on ζ and δ provided by the world average of the positron-polarization compar-

isons [Eq. (6)] are illustrated in Fig. 7 (bold line). They are compared to bounds resulting from other measurements on semileptonic transitions: the absolute polarization of electrons from Gamow-Teller decays[6] (bold dashed line) and the neutron β asymmetry and lifetime[27] (bold dotted line). The bounds deduced from the published ^{19}Ne β asymmetry[28] and corresponding ft value[29] yield constraints similar to the ones obtained from neutron decay and are not represented in Fig. 7. It may be interesting to note here that both the as-yet unpublished data on the ^{19}Ne β asymmetry[30,31] and those on the neutron β asymmetry[32] seem incompatible with $\delta=\zeta=0$. For illustration's sake only, we indicate in Fig. 7 also the constraint deduced from the measurement of the end-point positron spectrum in the decay of polarized muons[33] (dashed line); in some scenarios this constraint cannot be compared to those deduced from semileptonic transitions.[9,34] We stress also the complementarity of the constraints we report here on right-handed currents with those deduced from the observation of neutrinos from the supernova SN 1987A,[35] which excluded some particular region in the $\zeta\delta$ parameter space.

In the absence of phase-space effects introduced by neutrino mass, the interpretation of our result in nonmanifest left-right symmetric models, considered by Herczeg[9] or by Langacker and Sankar,[34] requires only a suitable modification of the definition of the parameters δ and/or ζ. It should be stressed, however, that some of these models invalidate the tight constraints readily deduced from K_L/K_S mass difference or muon decay and so emphasize the interest in the type of investigations on semileptonic transitions we report. The information derived from this work is also related to that deduced from the absence of neutrino less double-beta decay. However, our constraints do not rely on the Majorana character of the neutrino, which has to be assumed in the interpretation of the double-beta decay experiments.

The prospects for further improvement of the constraints on the product $\zeta\delta$ by improved precision experiments of the ratio P_F/P_{GT} are good: As discussed in this paper, our experiment is not limited by systematic uncertainties and the effect of uncontrolled recoil-order corrections is, moreover, still negligible at the actual level of precision. As, however, rather stringent limits were obtained on the parameter ζ from the unitarity constraint of the Kobayashi-Maskawa-Cabibbo matrix,[36,37] it may be preferable to concentrate efforts on constraining other combinations of the parameters ζ and δ. Relative polarization measurements from polarized nuclei, which constrain the sum $\zeta+\delta$, have been readily considered in this context,[38] and at least two such measurements are in progress.[39]

Our result also provides constraints on scalar and tensor couplings absent in the standard model. Denoting the corresponding coupling constants (assumed real) by C_S and C_S', and C_T and C_T', respectively, and assuming $C_V=C_V'$ and $C_A=C_A'$, our result yields [cf. Eq. (2)]

$$(C_S+C_S')/C_V-1.001[(C_T+C_T')/C_A]$$
$$=-0.0014\pm0.0210\ (90\%\ \text{C.L.})\ .$$

The result of Wichers *et al.*[7] provides

$$(C_S+C_S')/C_V-0.998[(C_T+C_T')/C_A]$$
$$=0.0138\pm0.0346\ (90\%\ \text{C.L.})\ .$$

Combining these two constraints, we obtain then

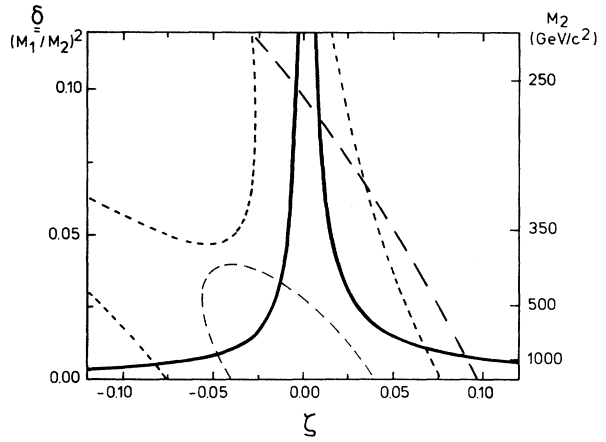

FIG. 7. Constraints, at 90% confidence, on the squared mass ratio δ and the mixing angle ζ of the two bosons in the left-right symmetric model, deduced from the world average (this work and Ref. 7) in relative polarization measurements (bold line) and from other semileptonic experiments: β-polarization measurements (Ref. 6) (bold dashed line), neutron lifetime, and asymmetry measurements (Ref. 27) (bold dotted line). Also shown is the bound from the measurement of the end-point e^+ spectrum in muon decay (Ref. 33) (dashed line).

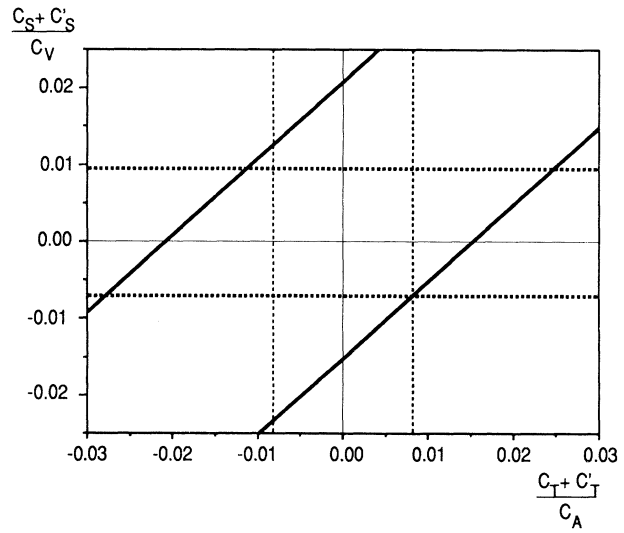

FIG. 8. Limits, at 90% confidence, on the real part of the scalar and tensor couplings, from this measurement combined with that of Wichers *et al.* (Ref. 7) (bold line). Also shown are the limits on scalar and tensor admixtures obtained recently in Refs. 40 and 41.

$$(C_S+C_S')/C_V-(C_T+C_T')/C_A$$
$$=0.0027\pm0.0179 \text{ (90\% C.L.)} . \quad (7)$$

This bound is shown in Fig. 8. Also shown is a limit on the scalar contribution deduced recently by Ormand, Brown, and Holstein[40] from the superallowed 0^+-0^+ transitions and a limit on the tensor contribution obtained by Boothroyd, Markey, and Vogel[41] from a least-squares adjustment of beta-decay data. This limit on the tensor coupling is, however, open to controversy because of its neglect of induced weak corrections and heavy dependence on internally inconsistent ^{22}Na-decay data (see also Ref. 42). Using the constraint obtained from the superallowed Fermi transitions,[40]

$$b_F=(C_S+C_S')/C_V=(1.2\pm5)\times10^{-3} ,$$

we find, from Eq. (7),

$$b_{GT}=(C_T+C_T')/C_A=-(1.5\pm12)\times10^{-3} .$$

In this context Poblaguev[42] recently proposed a nonzero value for the tensor coupling $b_{GT}\approx(4.2\pm1.6)\times10^{-3}$ on the basis of radiative pion-decay experiments. His value is in agreement with the constraint deduced from this experiment in conjunction with the existing limits on C_S.

ACKNOWLEDGMENTS

We have appreciated many useful discussions with M. Skalsey and J. van Klinken during the evolution of this measurement, and with B. Holstein on some aspects of the analysis. We thank L. Dick for the loan of the polarimeter magnet and gratefully acknowledge the contributions of the UCL cyclotron, mechanical, and electronic staff, far too numerous to mention, and without whom this project could not have been accomplished. We also thank M. Jacques for construction and maintenance of the target transport system, B. Tasiaux, D. Claes, L. Michel, and F. Vecchio Verderame for their assistance during various phases of the data acquisition, and D. Dedouaire for the loan of his laboratory in which the MgO pellets were prepared. This work was supported by the IISN (Interuniversity Institute of Nuclear Science, Belgium).

*Now at University of South Carolina, Columbia, SC 29208.

[1]P. Herczeg, in *Proceedings of the Conference on Weak and Electromagnetic Interactions in Nuclei, Heidelberg, 1986,* edited by H. V. Klapdor (Springer-Verlag, New York, 1987), p. 528; R. N. Mohapatra, *ibid.*, p. 493.
[2]J. C. Pati and A. Salam, Phys. Rev. Lett. **31**, 661 (1973).
[3]J. C. Pati and A. Salam, Phys. Rev. D **10**, 275 (1974).
[4]R. N. Mohapatra and J. C. Pati, Phys. Rev. D **11**, 566 (1975); **11**, 2558 (1975).
[5]M. A. B. Bég, R. V. Budny, R. Mohapatra, and A. Sirlin, Phys. Rev. Lett. **38**, 1252 (1977).
[6]J. van Klinken, K. Stam, W. Z. Venema, and V. A. Wichers, Phys. Rev. Lett. **50**, 94 (1983).
[7]V. A. Wichers, T. R. Hageman, J. van Klinken, and H. W. Wilschut, Phys. Rev. Lett. **58**, 1821 (1987).
[8]J. D. Jackson, S. B. Treiman, and H. W. Wyld, Nucl. Phys. **4**, 206 (1957).
[9]P. Herczeg, in *Proceedings of the International Symposium on Fundamental Symmetries in Nuclei and Particles, Caltech, Pasadena, 1989* (World Scientific, Singapore, 1990).
[10]M. Skalsey, T. A. Girard, D. Newman, and A. Rich, Phys. Rev. Lett. **49**, 708 (1982); M. Skalsey, T. A. Girard, and A. Rich, Phys. Rev. C **32**, 1014 (1985).
[11]J. Van House and P. W. Zitzewitz, Phys. Rev. A **29**, 96 (1984).
[12]T. A. Girard, A. S. Carnoy, J. Deutsch, R. Prieels, and M. L. Schmidt, Z. Phys. A **330**, 51 (1988).
[13]R. Prieels, in *Proc. XXIV Rencontre de Moriond,* January 1989, edited by O. Fackler and J. Tran Thanh Van (Editions Frontières, Gif-sur-Yvette, 1989), p. 287.
[14]A. S. Carnoy *et al.*, Phys. Rev. Lett. **65**, 3249 (1990).
[15]M. Skalsey, D. W. Holdsworth, D. A. L. Paul, and A. Rich, Phys. Rev. C **39**, 986 (1989), and references therein.
[16]S. Berko and H. N. Pendleton, Annu. Rev. Nucl. Part. Sci. **30**, 543 (1980).
[17]C. Bouchiat and J. M. Lévy-Leblond, Nuovo Cimento **23**, 193 (1963).
[18]S. Orito, K. Yoshimura, T. Haga, M. Minowa, and M. Tsuchiaki, Phys. Rev. Lett. **63**, 597 (1989).
[19]L. Dick, L. Feuvrais, L. Madansky, and V. L. Telegdi, Phys. Lett. **3**, 326 (1963).
[20]W. Brandt and R. Paulin, Phys. Rev. Lett. **21**, 193 (1968).
[21]R. Paulin and G. Ambrosino, J. Phys. (Paris) **29**, 263 (1968).
[22]D. H. Wilkinson, Nucl. Phys. **A209**, 470 (1973).
[23]B. R. Holstein, Phys. Rev. C **16**, 1258 (1977).
[24]T. A. Girard, Phys. Rev. C **27**, 2418 (1983).
[25]F. P. Calaprice and B. R. Holstein, Nucl. Phys. **A273**, 301 (1976).
[26]F. Ajzenberg-Selove, Nucl. Phys. **A490**, 1 (1988).
[27]D. Dubbers, W. Mampe, and J. Döhner, Europhys. Lett. **11**, 195 (1990).
[28]F. P. Calaprice, S. J. Freedman, W. C. Mead, and H. C. Vantine, Phys. Rev. Lett. **35**, 1566 (1975).
[29]F. Ajzenberg-Selove, Nucl. Phys. **A392**, 1 (1983).
[30]D. Schreiber, Ph.D. thesis, Princeton University, 1983.
[31]J. Deutsch, in *Proceedings of the Fundamental Symmetries and Nuclear Structures, Santa Fe, New Mexico, 1988,* edited by J. N. Ginocchio and S. P. Rosen (World Scientific, Singapore, 1989).
[32]Yu.V. Gaponov, N. B. Shul'gina, and P. E. Spivak, Phys. Lett. B **253**, 283 (1991), and references therein.
[33]A. Jodidio, B. Balke, J. Carr, G. Gidal, K. A. Shinsky, H. M. Steiner, D. P. Stoker, M. Strovink, R. D. Tripp, B. Gobbi, and C. J. Oram, Phys. Rev. D **34**, 1967 (1986); **37**, 237(E) (1988).
[34]P. Langacker and S. U. Sankar, Phys. Rev. D **40**, 1569 (1989).
[35]R. Barbieri and R. N. Mohapatra, Phys. Rev. D **39**, 1229 (1989).
[36]J. Deutsch, Acta Phys. Hung. **68**, 129 (1990).
[37]D. H. Wilkinson, Phys. Lett. B **241**, 317 (1990); **242**, 548(E) (1990).

[38]P. A. Quin and T. A. Girard, Phys. Lett. B **229**, 29 (1989).
[39]M. Allet *et al.*, proposal for an experiment at PSI, Switzerland (proposal No. Z-90-07.1); N. Severyns *et al.*, proposal for an experiment at UCL, Louvain-la-Neuve, Belgium (proposal No. PH79-90).
[40]W. E. Ormand, B. A. Brown, and B. R. Holstein, Phys. Rev. C **40**, 2914 (1989).
[41]A. I. Boothroyd, J. Markey, and P. Vogel, Phys. Rev. C **29**, 603 (1984).
[42]A. A. Poblaguev, Phys. Lett. B **238**, 108 (1990).